Spectrochimica Acta Part A: Molecular and Biomolecular Spectroscopy 324 (2025) 124939

Contents lists available at ScienceDirect

Spectrochimica Acta Part A:
Molecular and Biomolecular Spectroscopy

journal homepage: www.journals.elsevier.com/spectrochimica-acta-part-a-molecular-and-biomolecular-spectroscopy

Guanosine hydrogels in focus: A comprehensive analysis through mid-infrared spectroscopy

Valentina Notarstefano [a,*,1], Alessia Pepe [a,1], Francesca Ripanti [a], Federica Piccirilli [b], Lisa Vaccari [b], Paolo Mariani [a]

[a] Università Politecnica delle Marche, Department of Life and Environmental Sciences, Via Brecce Bianche, Ancona, 60131, Italy
[b] Elettra Sincrotrone Trieste, S.S. 14 - km 163.5, Basovizza, 34149, Italy

HIGHLIGHTS

- ATR-FTIR spectroscopy unveils new insights on the formation of guanosine hydrogels.
- Different cations (K^+ and Na^+) affect the stability of the promoted quadruplex structures.
- The aggregation properties of quadruplexes can be tuned by varying Gua:GMP molar ratio.

GRAPHICAL ABSTRACT

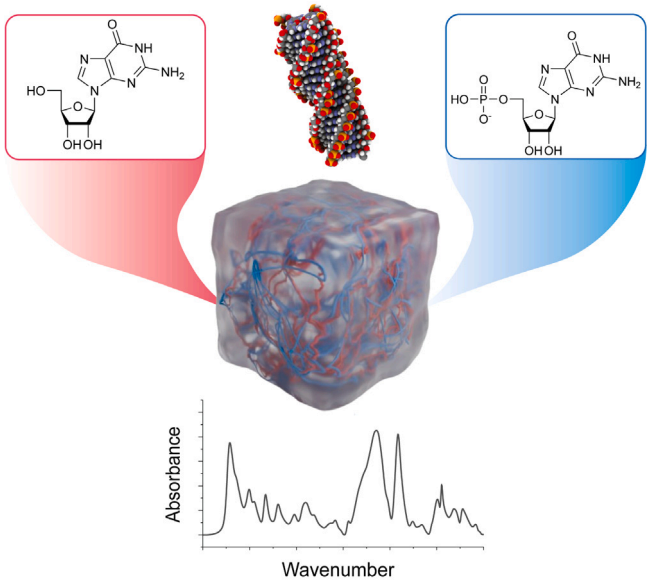

ARTICLE INFO

Keywords:
ATR-FTIR
G-quadruplex
Hydrogel
Biophysical characterization

ABSTRACT

Guanosine nucleosides and nucleotides have the peculiar ability to self-assemble in water to form supramolecular complex architectures from G-quartets to G-quadruplexes. G-quadruplexes exhibit in turn a large liquid crystalline lyotropic polymorphism, but they eventually cross-link or entangle to form a densely connected 3D network (a molecular hydrogel), able to entrap very large amount of water (up to the 99% v/v). This high water content of the hydrogels enables tunable softness, deformability, self-healing, and quasi-liquid properties, making them ideal candidates for different biotechnological and biomedical applications.

In order to fully exploit their possible applications, Attenuated Total Reflection-Fourier Transform InfraRed (ATR-FTIR) spectroscopy was used to unravel the vibrational characteristics of supramolecular guanosine structures. First, the characteristic vibrations of the known quadruplex structure of guanosine 5′-monophosphate,

* Corresponding author.
E-mail address: v.notarstefano@univpm.it (V. Notarstefano).
[1] These two authors contribute equally to the work.

https://doi.org/10.1016/j.saa.2024.124939
Received 29 March 2024; Received in revised form 27 June 2024; Accepted 5 August 2024
Available online 8 August 2024
1386-1425/© 2024 The Author(s). Published by Elsevier B.V. This is an open access article under the CC BY-NC-ND license (http://creativecommons.org/licenses/by-nc-nd/4.0/).

potassium salt (GMP/K), were investigated: the identified peaks reflected both the chemical composition of the sample and the formation of quartets, octamers, and quadruplexes. Second, the role of K^+ and Na^+ cations in promoting the quadruplex formation was assessed: infrared spectra confirmed that both cations induce the formation of G-quadruplexes and that GMP/K is more stable in the G-quadruplex organization. Finally, ATR-FTIR spectroscopy was used to investigate binary mixtures of guanosine (Gua) and GMP/K or GMP/Na, both systems forming G-hydrogels. The same G-quadruplex-based structure was found in both mixtures, but the proportion of Gua and GMP affected some features, like sugar puckering, guanine vibrations, and base stacking, reflecting the known side-to-side aggregation and bundle formation occurring in these binary systems.

1. Introduction

Guanosine nucleosides and nucleotides are known to self-assemble in water to form supramolecular complex architectures [1]. This is a peculiar association since, among nucleobases, only guanine is able to interact even in a large water environment (up to 99%) with other three guanines, leading to the formation of a supramolecular aggregate known as G-quartet. G-quartets in turn stack one on top of the other to form chiral columnar structures named G-quadruplexes. Several low-molecular weight guanine derivatives are present in nature and are involved in this phenomenon: in this paper, guanosine (Gua) and guanosine 5′-monophosphate (GMP) were considered. The G-quartet is a planar structure derived from non-conventional H-bonds, called Hoogsteen scheme, among four guanine molecules [2]. In this arrangement the phosphate groups of GMP are in the external part of the structure. By the regular π–π stacking of tetramers, other ordered structures form in water in the presence of alkali metal cations: first the G-octamer (a dimer of G-quartets), afterwards the G-dodecamer (a trimer of G-quartets), and finally the G-quadruplex. The G-quadruplex supramolecular organization is similar to that of DNA, but the helix is four-stranded and the backbone is absent. Two points can be underlined: each G-quartet is rotated of around 30° with respect to the next one [1]; the stacking distance between the G-quartets, as derived from X-ray diffraction experiments [3], is around 3.34 Å, similar to the one observed in the DNA molecule.

Although G-quadruplexes can be observed in the telomeric region of the chromosome into the cells [4], there is a double possibility to prepare stable G-quadruplexes in solution. At one side, GMP in water at concentrations larger than 10% w/v and in the presence of K^+ or Na^+ forms stiff G-quadruplexes that organize in columnar liquid crystalline lyotropic phases of hexagonal and cholesteric type [5]. The stability and structural properties of the phases were related to the phosphate negative charges on the G-quadruplex surface, which provide lateral repulsive forces between neighbor G-quadruplexes. At the other side, we recently demonstrated that, by replacing a fraction of GMP with Gua at a proper molar ratio, the G-quadruplexes maintain their architecture, but the induced flexibility and the enhanced contribution of attractive van der Waals forces determine G-quadruplex cross-linking and entanglement, and then the formation of a densely connected 3D hydrogel network [1]. The Gua molecule holds the key to understand such behavior since, being uncharged, insoluble [6], and still able to form G-quartets, it controls the G-quadruplex properties [7].

A last observation concerns the G-quadruplex formation, which occurs when guanine molecules are dissolved in water in the presence of alkaline metal ions. The role of the cation is crucial for the stability of the G-quartets (through the coordination of the oxygen atoms in the G-quartet central cavity) and of the G-quadruplexes, through the coordination of eight oxygen atoms in two stacked G-quartets. Not all the cations are effectively able to fit the G-quadruplex cavity, hence they were evaluated according to their stabilizing ability [8] and classified as follows:

$$K^+ > Rb^+ > Na^+ > Cs^+ = Li^+$$

In particular, considering two forms of GMP, i.e., the potassium (GMP/K) and the sodium (GMP/Na) salts, it has been observed that both of them are able to originate the G-hydrogel, but the presence of potassium ions induces more stable (more longer) G-quadruplexes. Probably, the size of the cation and the dehydration energy plays an important role in determining the bonding strength to the O6 of staked guanines.

Among the others, the absence of a backbone, the Gua-GMP replacement, and the counterion coordination strongly control the self-assembling process, the G-quadruplex stability and, as a consequence, the hydrogel properties. Because of the several and unique applications that have been suggested for the G-hydrogel, a comprehensive analysis of intramolecular and intermolecular interactions, including hydrogen bonds, cation–O6 coordinations, π–π interactions, and base stacking is mandatory.

In this paper, Attenuated Total Reflection-Fourier Transform InfraRed (ATR-FTIR) spectroscopy was used to identify vibrational modes of molecular bonds, functional groups, and intra- and intermolecular interactions characteristic of guanosine hydrogels. The systematic description of these vibrational fingerprint will let obtain some reference parameters to be monitored when setting up applications of guanosine hydrogels.

2. Experimental

2.1. Sample preparation

The GMP/K was prepared by using ion-chromatography exchange, starting from a solution of GMP/Na (purchased from Sigma Aldrich). The eluted solution was precipitated by adding a water/ethanol mixture at 1:3 ratio, centrifuged at 4000 rpm for 15 min. Pellets were lyophilized overnight and then stocked at −20 °C. GMP/Na was used as it is.

GMP/K and GMP/Na quadruplexes were prepared by adding to the lyophilized derivatives the proper amount of milli-Q water. The water sample concentration was 200 mg/ml.

G-hydrogels were prepared at different Gua:GMP/K and Gua:GMP/Na molar ratio (3:2, 1:1, 1:2, 1:4) and at a water composition of 95% v/v. For hydrogel preparation, two stock solutions of Gua and GMP (GMP/K or GMP/Na), 150 mg/ml and 200 mg/ml respectively, were prepared. The right volumes of the two solutions were mixed in a vial tube and then milli-Q water was added to reach the desired hydration amount. To improve the kinetic of the hydrogel formation and to homogenize the samples, the mixtures were heated in a thermo-bath at 80 °C for a few minutes. By cooling down the samples, a stable and transparent hydrogel forms at room temperature. Samples were stoked at 4 °C and they remain stable also for one month. Note that the G-hydrogel 3:2 is stable only for a few hours in contrast with the other samples.

2.2. ATR-FTIR measurements

ATR-FTIR measurements were carried out at the IR SISSI beamline, Elettra Sincrotrone Trieste (Trieste, Italy), by employing a MIRacle Single Reflection ATR box (PIKE Technologies) with a diamond crystal, mounted on a Vertex 70 interferometer (Bruker Optics, Ettlingen, Germany) equipped with a deuterated triglycine sulfate detector. Samples

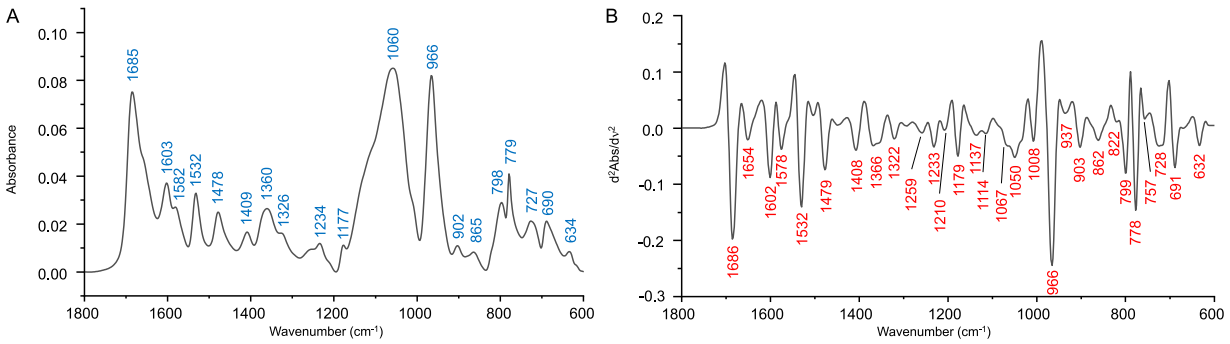

Fig. 1. Absorbance (A) and second derivative (B) spectral profiles of the GMP/K sample. The center position of the most prominent bands are reported.

deposited onto the diamond crystal were purged with a continuous stream of nitrogen gas. IR spectra were collected every 10 s until complete removal of the free water content, as monitored by the disappearance of the band at ~2100 cm^{-1}, indeed relative to the free water molecules. This time evolution is shown in Fig. A.14. For each sample, three spectra were acquired in reflection mode in the spectral range 4000–400 cm^{-1} (spectral resolution 4 cm^{-1}, 256 scans). A background spectrum was collected on the clean diamond crystal, before each sample measurement. All IR spectra were converted into Absorbance mode, interpolated in the spectral range 1800–600 cm^{-1}, two-points baseline linear fitted, and converted in second derivative mode (OPUS 7.5 software, Bruker Optics).

2.3. Infrared data analysis

The curve fitting in some spectral regions of interest was performed upon local straight baseline correction and vector normalization. The number and position of the underlying subpeaks were identified by the analysis of second derivative minima and fixed during the fitting procedure by means of Gaussian functions (OriginPro 2023b, OriginLab Corporation). The detailed fitting results are reported in Appendix C.

3. Results and discussion

IR experiments were performed by analyzing at first the characteristic vibrational spectra of the quadruplex structure obtained by GMP/K in water, then by evaluating the role of K^+ and Na^+ cations in promoting the quadruplex formation, and finally by considering binary mixtures of Gua and GMP/K and GMP/Na, which form G-hydrogels. The section is divided into several paragraphs, each focused on a significant spectral marker and its interpretation for the analyzed condition, and repeated for all the considered systems.

3.1. Mid-IR spectrum of GMP/K quadruplexes

To assess the characteristic vibrations of the known quadruplex structure, the spectral features of GMP/K were evaluated by studying its mid-IR spectrum. Fig. 1 displays the absorbance and second derivative spectral profiles obtained. The peaks identified from absorbance and second derivative spectra reflect the chemical composition of the sample, hence comprise the vibrational modes of guanine, ribose, and phosphate groups. In addition, some features were ascribable to the formation of quartets, octamers, and quadruplexes. The detailed assignments and interpretation of the accounted bands are described in the subsequent sections.

3.1.1. The C6=O6···N1–H

The first relevant and the most pronounced peak is centered at ~1685 cm^{-1} and is related to the stretching mode of the C6=O6 ($\nu_{C6=O6}$) of guanine. It has been reported that this peak arises at 1655–1670 cm^{-1} in single stranded DNA. When guanosines undergo self-association, forming a tetramer through Hoogsteen-type G–G interactions, this carbonyl group becomes engaged in a hydrogen bond, causing a shift in this band to higher wavenumbers, as in the present case [9–11]. Several factors affect the position of the $\nu_{C=O}$ peak. First, it is known that the $\nu_{C=O}$ peak in aromatic carbonyl units appears approximately 60 cm^{-1} lower (~1665 cm^{-1}) than that in saturated carbonyl units (~1720 cm^{-1}). This is due to conjugation, the partial overlap between the aromatic ring p-type orbitals extending above the molecular plane, and the carbonyl group's p-type orbital directed towards the aromatic ring. This conjugation diminishes the strength of the C=O bond, reducing its force constant and resulting in an average peak position shift of about 30 cm^{-1} [12].

Moreover, the significant shift of the $\nu_{C6=O6}$ band reflects the formation of hydrogen bonds on this carbonyl, the cation coordination, and the stacking interaction between contiguous G-quartet planes [9,13–15]. The first of these two factors relies on the formation of G-quartets. However, in this structure, hydrogen bonds polarize the π-electrons of single GMP monomers: this leads to the formation of resonance forms for all the four monomers, which display cyclic [4n+2] π-electrons delocalizations [16]. As a result, in the G-quartet the C=O groups display a greater length (1.223 Å) with respect to the aromatic carbonyl of the monomer (1.208 Å) [16], thus leading, as a matter of fact, to a decrease in the absorption frequency. Moreover, in the presence of cations complexed to the G-quartet, the polarization of ring π-electrons is even greater, leading to a further increase in carbonyl bond length both with one K^+ (1.241 Å) and with two K^+ (1.258 Å) [16]. Hence, the blue shift from ~1665 cm^{-1} of aromatic carbonyls to ~1690 cm^{-1} of G-quadruplexes does not seem to be ascribable to hydrogen bonding and cation coordination at the basis of G-quartet formation.

Hence, since Hoogsteen hydrogen bonding and metal coordination induce C=O bond lengthening, the coupling effects of quartets should be also considered, like base stacking, which are able to delocalize vibrations among multiple bases within the ordered structure of quadruplexes [13]. Indeed, as in the present case, GMP quadruplex formation induced a blue shift of the $\nu_{C6=O6}$, with respect to aromatic carbonyls of GMP alone. This result, besides being consistent with previous literature [9,15,17–20], has not been thoroughly investigated and explained. Price and colleagues suggest that the blue shift of the peak assigned to $\nu_{C6=O6}$ is due to the coupling between G-quartets, a shift that they report to be ~+20 cm^{-1} [13].

3.1.2. The guanine base

The peak centered at ~1603 cm^{-1} is attributed to the guanine base stretching/deformation vibrations [14,21]. It has been reported that the IR spectrum of monomeric GMP displays the absorption assigned to the

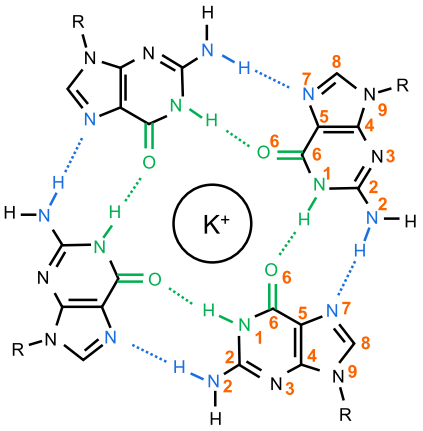

Fig. 2. Hoogsteen type hydrogen bonds between C6=O6 and N1–H groups (green) and between N7 and N2–H groups (blue).

guanine ring at ~1570–1580 cm^{-1} [21,22]. In the present case, the absorption is significantly blue shifted: a similar shift (up to ~1593 cm^{-1}) has been ascribed as a signal of the GMP quadruplex formation [11,21]. Not only the shift, but also the intensity of this band seems to be quantitatively related to the formation and stability of quadruplexes, as suggested by its decrease upon an increase of temperature [11]. Moreover, the intensity of this band upon G-quadruplex formation decreases with respect to single GMP spectrum, probably due to an hypochromic effect related to the π-π electron interaction of the stacked guanine bases [21].

Next to this peak, a shoulder, centered at 1582 cm^{-1} in absorbance mode and at 1578 cm^{-1} in second derivative mode, is clearly visible. Since both the infrared bands at 1603 cm^{-1} and at 1582 cm^{-1} can be assigned to C=C and C=N guanine ring deformations, it can be hypothesized that multiple forms of GMP coexist in the sample, from single monomers, to G-quartets, to G-octamers, to G-quadruplexes. Moreover, the contribution of the terminal G-quartet of cylinders may also play a part in the presence of both these peaks.

The peak found at 1360 cm^{-1} in absorbance mode is also ascribable to guanine vibration modes: in particular, it is assigned to the stretching vibrations involving C8 (ν_{C8-N9} and $\nu_{C8=N7}$) [22,23]. In second derivative mode, this peak appears divided into a doublet, with a major contribution at 1366 cm^{-1} and a shoulder at 1358 cm^{-1}.

3.1.3. The N7···N2–H

Besides the Hoogsteen type hydrogen bonds between C6=O6 and N1–H groups, the involvement of GMP in tetrads also relies on the formation of a hydrogen bond between N7 and N2-H groups (Fig. 2).

There is consensus that the existence of the N7···N2–H hydrogen bond is evidenced by the emergence of a new absorption located at ~1535 cm^{-1}, which is almost absent in the spectrum of isolated deoxyguanosine 5′-monophosphate (dGMP) and that is considered indicative of the formation of a helical structure [9,10,21]. This is also confirmed by the evidence that a temperature-induced dissociation of G-quartets determines a decrease in intensity of this band [11].

Moreover, the formation of a hydrogen bond involving the N7 atom causes a red shift of the band assigned to the bending vibration of N7=C8–H ($\delta_{N7=C8-H}$): indeed, in single GMP, or in Watson–Crick pairing, this band is centered at ~1496 cm^{-1}, while here it is at ~1480 cm^{-1}, reflecting an interaction occurring on the N7 site [9,24].

3.1.4. Sugar puckering

In literature, it has been reported that GMP quartets are stacked following a head-to-tail organization, which leads to the formation of a chiral cylinder, thanks to a peculiar sugar puckering along the helical strand that sees alternating C2′-*endo* and C3′-*endo* conformations [11,25,26]. In fact, it has been described that the presence of chiral sugars linked to nucleobases determines the formation of two diasterotopic faces in each G-quartet (a 'head' and a 'tail') [27]. In contrast with right-handed B-form and A-form helices, which are known to contain only C3′-*endo* and C2′-*endo* respectively, this GMP helix, displaying alternating sugar conformations, is in this sense similar to the left-handed Z-DNA helix [25]. This geometry is crucial, since the alternating sugar puckering has a role in the stabilization of the helix via P–O^-···H–O2/3′ hydrogen bonds along the strand, which recall the phosphodiester bonds in polynucleotides [11].

The C2′-*endo* (S type) conformation is characterized by two infrared bands centered at ~865 cm^{-1} and ~805 cm^{-1}, while the C3′-*endo* (N type) absorbs at ~838 cm^{-1} [9,10]. Here, the second derivative spectrum clearly shows the presence of three peaks: 862 cm^{-1}, 822 cm^{-1}, and 799 cm^{-1}, suggesting the presence of both C3′-*endo* and C2′-*endo* conformations in the analyzed samples.

The band centered at 1409 cm^{-1} is less informative of the sugar conformation. It has been reported that the center of this band oscillates, based on the conformation of the deoxyribose in the molecule, between 1425 cm^{-1} (B-DNA), 1418 cm^{-1} (A-DNA), and 1408 cm^{-1} (Z-DNA) [24,28]. As regards the ribose, the in-plane vibrations of C2′-OH in RNA are reported to be in the spectrum at ~1400 cm^{-1} [22,24]. The absorbance at 1409 cm^{-1} of the present samples seems to be closer to the one of Z-DNA, possibly due to the shared alternating sugars conformations forming the helix.

3.1.5. Phosphate groups

Phosphate groups also play a crucial role in stabilizing the GMP helical structure. In the present case, a prominent absorbance band at 1060 cm^{-1} was found, corresponding to the 1067 cm^{-1} and 1050 cm^{-1} second derivative peaks. The symmetric stretching vibration of phosphate groups in double-stranded nucleic acids is found at ~1090 cm^{-1} [10,24]: this bands is reported to red shift and decrease in intensity upon melting of the double helix [10]. Moreover, some researchers compared the experimental and computed spectra of guanosine species: the $\nu_{P=O}$ band was centered at 1080 cm^{-1} in $d(G)_8$ samples (experimental), while in the computed spectra it was found at 1055 cm^{-1} for quadruplexes, at 1048 cm^{-1} for duplexes, and at 1043 cm^{-1} for single-strands [21].

Another prominent band is visible in the absorbance and second derivative spectra, centered at 966 cm^{-1}. The assignment of this band is often referred to as 'backbone vibration' in DNA/RNA, and it is related to the phosphate-deoxyribose/ribose skeletal motions [29]; however, in this case, no real backbone is present, since there is a lack of a proper phosphodiester chain, but it can be anyway assigned to the PO_3^{2-} group vibration [23,30].

For completeness, Gua and GMP powder infrared spectra were also acquired, in order to validate the obtained results, and reported in Fig. B.15.

3.2. G-quadruplexes made by GMP/K and GMP/Na: a mid-IR spectral comparison

As previously discussed, the presence of a monovalent alkaline cation is crucial in the self-assembly of G-quadruplexes. Indeed, if cations are not added to the solution, only GMP monomers are present [8,27]. Alkaline cations coordinate with the oxygen atoms in the inner cavity between G-quartets, participating in the modulation of their stacking. The role of several ions has been investigated, but a major interest has been focused on K^+ and Na^+, since they are the most represented intracellular and extracellular ions respectively [8,31–33].

The different cation dimensions and hydration shell size determine a cation-specific formation of G-quadruplexes, with the ionic radius being crucial in stabilizing the structure: Na^+, with a ionic radius of 0.95 Å, has proper dimensions to coordinate the four O6 of the

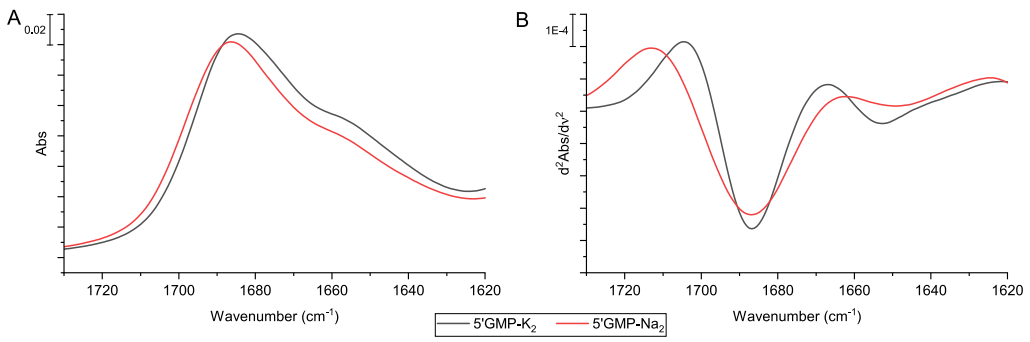

Fig. 3. Comparison of the spectral profiles (A, absorbance; B, second derivative) of GMP/K (black) and GMP/Na samples, with a focus on the 1730–1620 cm^{-1} spectral region.

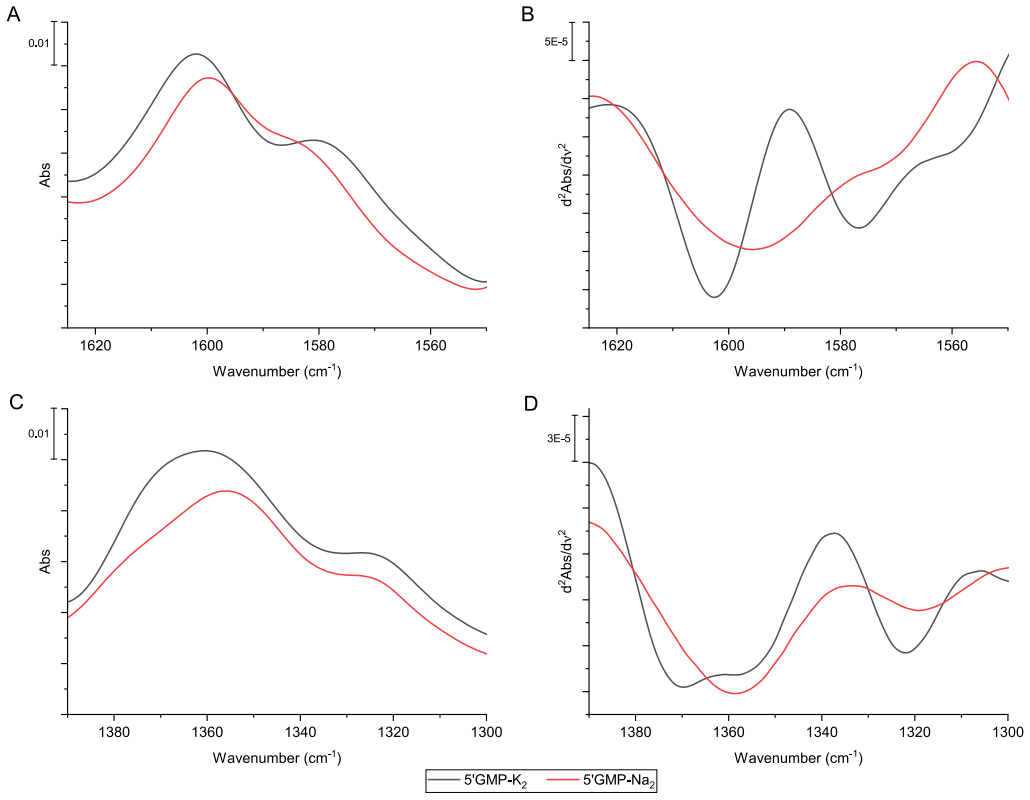

Fig. 4. Comparison of the spectral profiles (A,C, absorbance; B,D, second derivative) of GMP/K (black) and GMP/Na samples, with a focus on the 1625–1550 cm^{-1} and 1390–1300 cm^{-1} spectral regions.

guanines, within the plane, while K^+, with a ionic radius of 1.33 Å, cannot be coordinated within the plane of a G-quartet, but there is evidence of its coordination with eight O6, hence involving two adjacent G-quartets [8,34]. As a consequence, Na^+ induces the formation of numerous and short cylinders, while K^+ positively modulates the elongation process, leading to the formation of long cylinders [8].

In this light, we compared the mid-IR spectra of GMP/K and GMP/Na, in order to assess if the previously characterized spectral markers could reflect the different cation employed for G-quadruplex formation.

3.2.1. *The C6=O6···N1–H*

First, we compared the 1730–1620 cm^{-1} spectral region, mostly represented by the peak assigned to the $\nu_{C6=O6}$ of guanine (Fig. 3). Given the convoluted nature of this band, a careful fit was performed: the $\nu_{C6=O6}$ subpeak was found to be centered at ~1686 cm^{-1} in GMP/K and at ~1688 cm^{-1} in GMP/Na with no significant changes of the intensity but with a slightly increased w (peak width). The detailed fitting results are reported in Fig. C.16 and Table C.1 in Appendix C.

As previously discussed, the position of this peak is sensitive to C=O bond lengthening following Hoogsteen hydrogen bonding, metal coordination, and base stacking effects; hence, these different band features reflect the different behavior of the two monovalent cations within the G-quadruplex structure. In particular, the resulted blue-shifted and broader GMP/Na than GMP/K suggests a different 3D arrangement promoted by the employed cation.

3.2.2. *The guanine base*

The main peak attributed to the guanine stretching/deformation vibrations and centered in GMP/K at 1603 cm^{-1} displayed a red shift in GMP/Na. Moreover, the shoulder previously centered at 1582 cm^{-1} appeared significantly lower (Fig. 4).

As suggested above, the presence of both the bands assigned to C=C and C=N guanine ring deformations could be ascribable to the coexistence of multiple organization forms of GMP: hence, the broader and less defined shape of these two peaks, especially in second derivative mode, may suggest a more inhomogeneous status of the GMP/Na sample. The fit of these two peaks provided a further insight into these

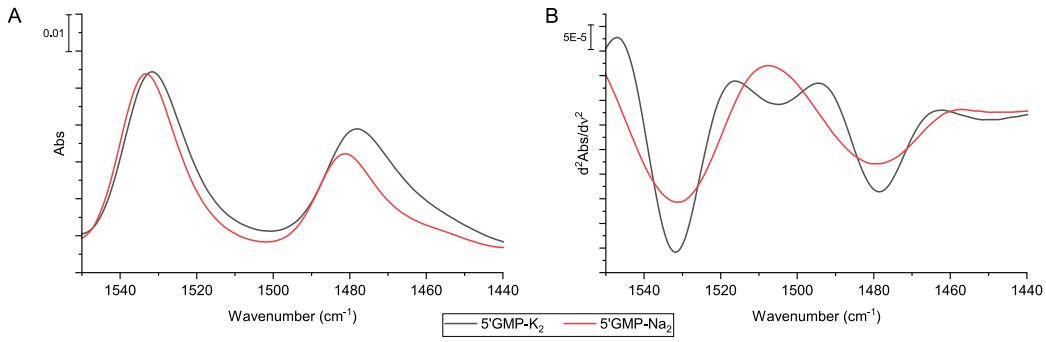

Fig. 5. Comparison of the spectral profiles (A, absorbance; B, second derivative) of GMP/K (black) and GMP/Na samples, with a focus on the 1550–1440 cm^{-1} spectral region.

spectral profiles, as reported in Fig. C.17 and Table C.1 in Appendix C. Indeed, in the case of GMP/K both the sub-peaks resulted to be shifted towards lower wavenumber, with a slightly increased intensity and a broader lineshape with respect to the GMP/Na ones. Moreover, the peak found in GMP/K at 1360 cm^{-1} in absorbance mode and at 1366 cm^{-1} in second derivative, assigned to guanine vibration modes, appeared red-shifted in GMP/Na.

Altogether, these results let confirm that also in GMP/Na quadruplexes are formed, but the shape and the intensity of the considered peaks provide information on a different stability status of the complexes, hence the π-π electron interaction of the stacked guanine bases is different when the monovalent cation changes. This is in accordance with available information on how the different cation size and hydration deeply affects the formation of G-quadruplexes, leading, for example, to the formation of shorter cylinders.

3.2.3. The N7···N2–H

The occurrence of a hydrogen bonding after the formation of G-quartets and involving the N7 atom is visible in the infrared spectrum by the two bands centered at 1532 cm^{-1} and at 1480 cm^{-1}.

In GMP/Na, both the peaks displayed a slight blue shift; the band assigned to $\delta_{N7=C8-H}$ also had a lower intensity (Fig. 5). Since in single GMP this band is reported to be centered at ~1496 cm^{-1}, the present blue shift may be consistent with the results of the previous section, which suggest a minor stability and a higher inhomogeneity of the GMP/Na system with respect to GMP/K.

3.2.4. Sugars puckering

The change in the employed monovalent cation to form G-quadruplexes seemed to affect the sugar puckering. In fact, in the GMP/Na second derivative infrared spectrum a broader peak at ~862 cm^{-1} (C2′-*endo*) was visible, but in place of the 822 (C3′-*endo*) and 799 (C2′-*endo*) cm^{-1} peaks, there was only one centered at ~807 cm^{-1} (Fig. 6). This latter peak may be attributable to a blue-shifted 799 cm^{-1} peak, suggesting that in GMP/Na the major sugar conformation is the C2′-*endo*.

3.2.5. Phosphate groups

In absorbance, the two spectral profiles of GMP/K and GMP/Na samples appeared almost superimposable in the 1200–915 cm^{-1} range, with a negligible increase of intensity of both the bands of interest. However, in second derivative, a smoother profile suggested a more inhomogeneous state of the GMP/Na sample, where the coexistence of diverse organization forms and the presence of shorter cylinders may determine a less defined signal in the whole spectrum (Fig. 7). In particular, while GMP/K displayed two second derivative peaks at 1067 cm^{-1} and 1050 cm^{-1}, here a single peak centered at 1057 cm^{-1} was found.

3.3. Gua:GMP/K quadruplexes: composition effects on the mid-IR spectra

It has been reported that a mixture of guanosine and GMP/K forms in water stable and transparent hydrogels, whose characteristics can be modified by tuning the proportions of the two components [1,35,36]. GMP/K is hydrophilic and highly soluble in water at neutral pH, while Gua is hydrophobic: as a consequence, when mixing the two species, GMP facilitates Gua solubilization and in turn Gua participates to the formation of G-quartets and promotes gelation, because of the reduced number of charges on the G-quadruplex surface [1]. As a result, when Gua partly replaces GMP, the quadruplex flexibility increases and the helix-to-helix repulsive interactions get weaker, thus leading to lateral aggregation and to the formation and stabilization of the hydrogel [1,7]. All these effects depend on the relative composition in Gua and GMP of the hydrogel; accordingly, changes in the spectral profiles of samples composed by different Gua:GMP ratios are expected.

3.3.1. The C6=O6···N1–H

Fig. 8 displays the spectral profiles of GMP/K, 1:4 Gua:GMP/K, 1:2 Gua:GMP/K, 1:1 Gua:GMP/K, and 3:2 Gua:GMP/K in the 1730–1620 cm^{-1} spectral range. The second derivative spectra of the five analyzed samples clearly showed a blue shift of the band centered at ~1685 cm^{-1}. This band was centered at 1686 cm^{-1} in GMP/K and 1:4 Gua:GMP spectra, at 1688 cm^{-1} in 1:2 Gua:GMP, at 1690 cm^{-1} in 1:1 Gua:GMP, and at 1691 cm^{-1} in 3:2 Gua:GMP. Hence, the center wavenumber linearly increased upon increasing Gua:GMP proportion, as shown in Fig. C.18A of Appendix C. The presence of this band in all the samples proves that Gua enters in quadruplex formation and is involved, as GMP, in Hoogsteen-type interactions, consistently with data reported in literature [1,35].

As previously described, the position of the $\nu_{C6=O6}$ band, centered in GMP/K at ~1685 cm^{-1}, is particularly sensitive to the formation of hydrogen bonds on this carbonyl group, to the stacking interactions between contiguous G-quartets, and to the metal coordination. In this comparison, samples share the same monovalent cation and the same Hoogsteen-type interactions, hence the differences found in the center position of the $\nu_{C6=O6}$ band have to be ascribed to the base stacking effects. As previously outlined, the observed blue shift of the $\nu_{C6=O6}$, with respect to aromatic carbonyls of GMP alone, can be attributed to Hoogsten hydrogen bonding, metal coordination, and base stacking. Here we highlight that the different composition in terms of Gua/GMP ratio gives rise to different quadruplex structures with diverse stacking interactions [13]. Indeed, the increasing amount of Gua in the mixture causes a further blue shift, suggesting that the inclusion of Gua affects the stacking of bases, possibly due to the onset of van der Waals interactions between quadruplexes, following the reduction of electrostatic repulsive forces, and the settlement of aggregates at a distance of closest contact [7]. In fact, the loss of some phosphate-related charges makes these binary quadruplexes more flexible and adhesive, facilitating side-by-side contacts and bundle formation, which may affect the interactions of quartets.

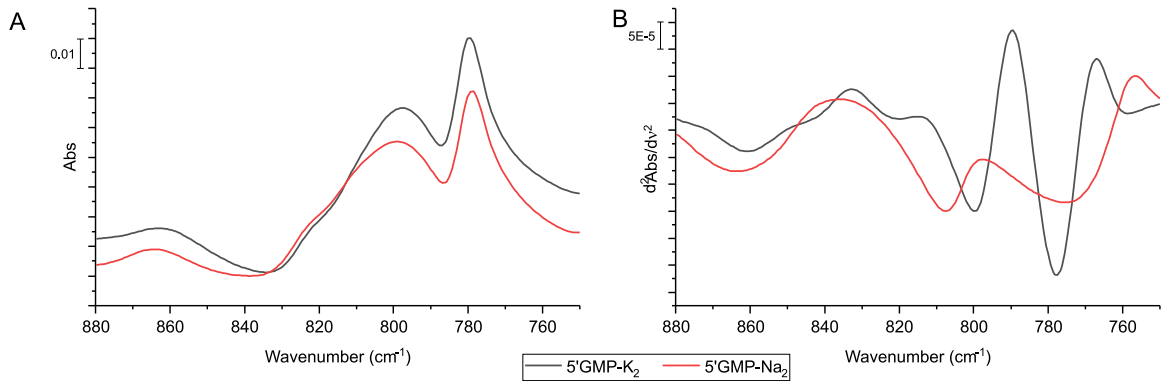

Fig. 6. Comparison of the spectral profiles (A, absorbance; B, second derivative) of GMP/K (black) and GMP/Na samples, with a focus on the 880–750 cm^{-1} spectral region.

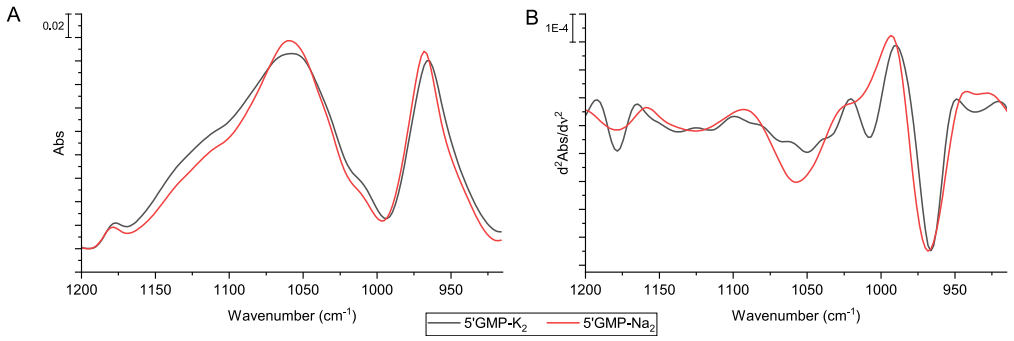

Fig. 7. Comparison of the spectral profiles (A, absorbance; B, second derivative) of GMP/K (black) and GMP/Na samples, with a focus on the 1200–915 cm^{-1} spectral region.

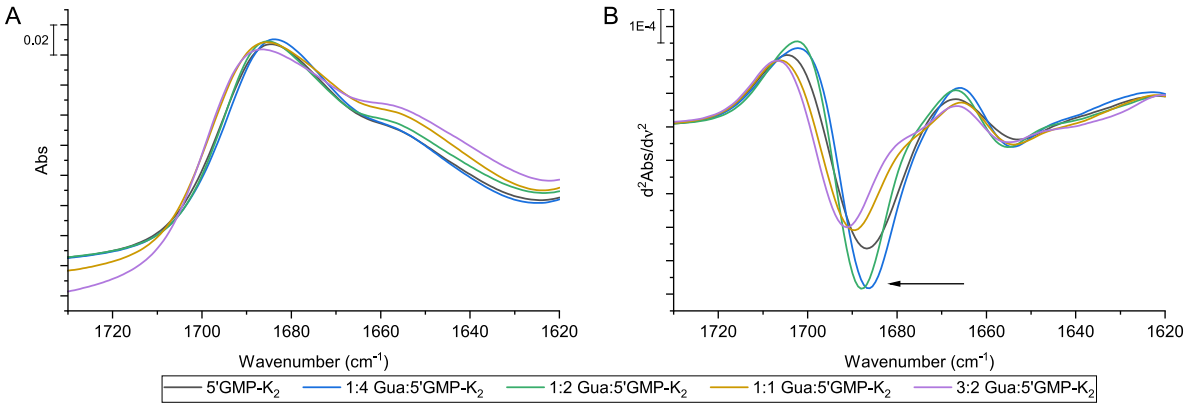

Fig. 8. Comparison of the spectral profiles (A, absorbance; B, second derivative) of GMP/K (black), 1:4 Gua:GMP/K (blue), 1:2 Gua:GMP/K (green), 1:1 Gua:GMP/K (yellow), and 3:2 Gua:GMP/K (purple) in the 1730–1620 cm^{-1} spectral region.

3.3.2. The guanine base

The peak centered in absorbance mode at 1603 cm^{-1} and in second derivative mode at 1602 cm^{-1}, attributed to the guanine base stretching/deformation vibrations, does not change its center position in relation to the Gua:GMP ratio, proving the formation of quadruplexes in all the analyzed samples. However, a change in its intensity is appreciable. Similarly, no changes were visible in the position of the shoulder at 1582 cm^{-1} in absorbance mode and at 1578 cm^{-1} in second derivative mode (Fig. 9A,B).

Considering the known relation between the intensity of these bands and the formation/stability of quadruplexes, a fit of the 1625–1550 cm^{-1} spectral region was performed, and the center positions of the principal peaks as a function Gua concentration are reported in Fig. C.18B,C,D of Appendix C. A slight increase in intensity of both the guanine-related bands was found as a function of the increase of the Gua:GMP ratio, suggesting a more pronounced side-to-side aggregation of quadruplexes, which could also affect the vibrational modes of the guanine bases forming the quartets.

As regards the 1400–1300 cm^{-1} spectral range, the second derivative clearly showed a separation of the doublet found in GMP/K, displaying two distinct peaks. Moreover, the peak at higher wavenumbers underwent a blue shift linearly correlated with the increasing Gua:GMP ratio as reported in Fig. 9C,D.

3.3.3. The N7···N2–H

The two bands centered at 1532 cm^{-1} and at 1480 cm^{-1}, related to the occurrence of a hydrogen bonding involving the N_7 atom are clearly visible also in binary Gua/GMP samples. No significant shift nor change in intensity of these bands were appreciable as a function of the Gua:GMP ratio (Fig. 10).

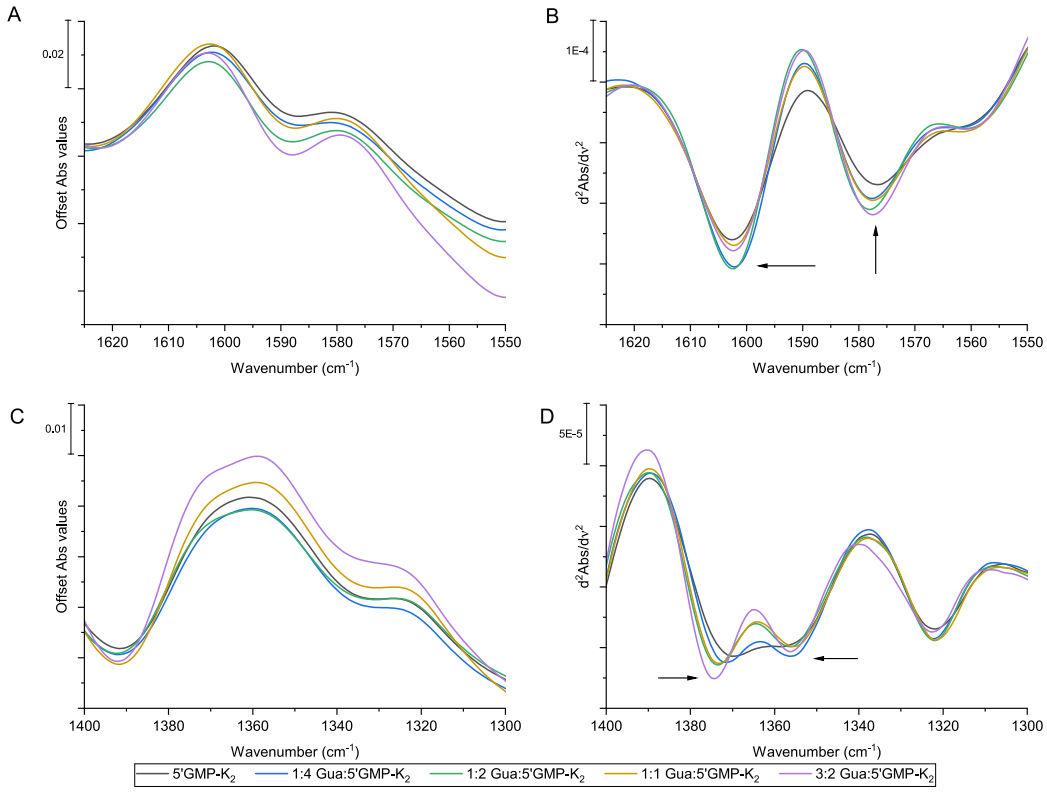

Fig. 9. Comparison of the spectral profiles (A, C, absorbance; B,D, second derivative) of GMP/K (black), 1:4 Gua:GMP/K (blue), 1:2 Gua:GMP/K (green), 1:1 Gua:GMP/K (yellow), and 3:2 Gua:GMP/K (purple) in the 1625–1550 cm^{-1} and 1400–1300 cm^{-1} spectral regions.

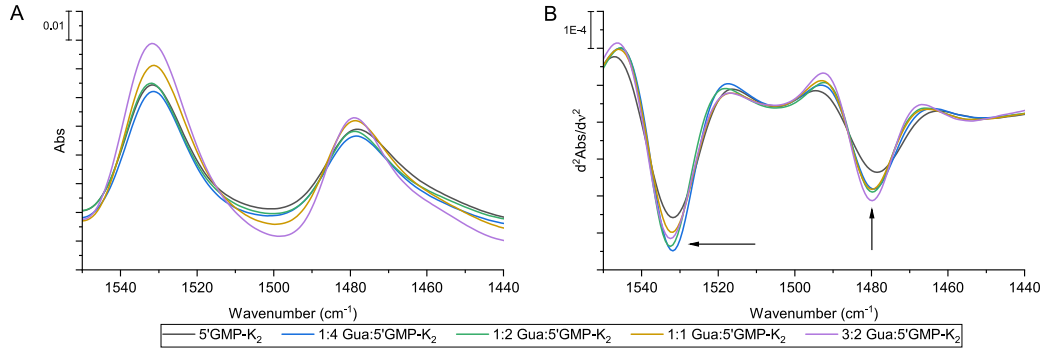

Fig. 10. Comparison of the spectral profiles (A, absorbance; B, second derivative) of GMP/K (black), 1:4 Gua:GMP/K (blue), 1:2 Gua:GMP/K (green), 1:1 Gua:GMP/K (yellow), and 3:2 Gua:GMP/K (purple) in the 1550–1440 cm^{-1} spectral region.

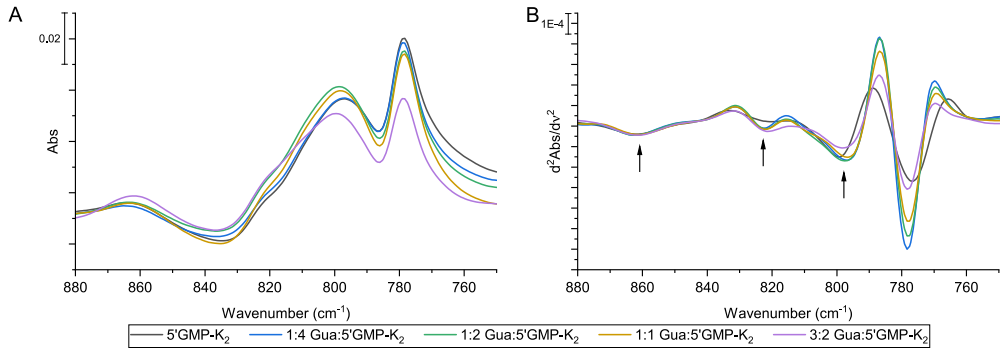

Fig. 11. Comparison of the spectral profiles (A, absorbance; B, second derivative) of GMP/K (black), 1:4 Gua:GMP/K (blue), 1:2 Gua:GMP/K (green), 1:1 Gua:GMP/K (yellow), and 3:2 Gua:GMP/K (purple) in the 880–750 cm^{-1} spectral region.

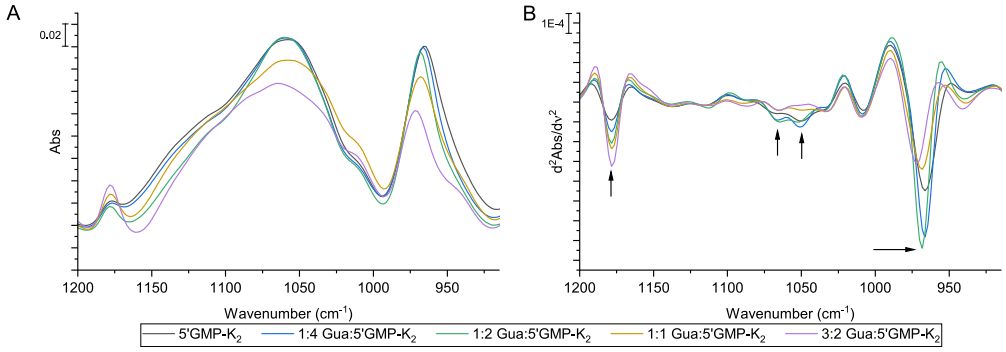

Fig. 12. Comparison of the spectral profiles (A, absorbance; B, second derivative) of GMP/K (black), 1:4 Gua:GMP/K (blue), 1:2 Gua:GMP/K (green), 1:1 Gua:GMP/K (yellow), and 3:2 Gua:GMP/K (purple) in the 1200–915 cm^{-1} spectral region.

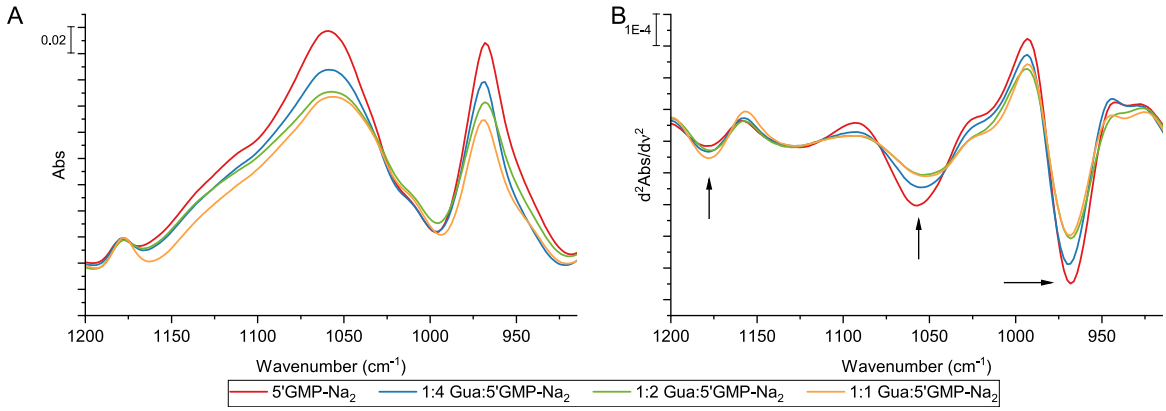

Fig. 13. Comparison of the spectral profiles (A, absorbance; B, second derivative) of GMP/Na (red), 1:4 Gua:GMP/Na (cyan), 1:2 Gua:GMP/Na (green), and 1:1 Gua:GMP/Na (orange) in the 1200–915 cm^{-1} spectral range.

3.3.4. Sugars puckering

As regards the C2′-*endo* conformation, the change in the Gua:GMP ratio did not affect the band at ~862 cm^{-1}, while a red shift from 799 cm^{-1} to ~796 cm^{-1} was found in all the binary Gua:GMP samples. The contribution of the ~822 cm^{-1} peak (C3′-*endo* conformation) to the IR spectrum showed to be more pronounced in all the binary Gua/GMP samples, and also its center position undergoes a red shift (Fig. 11).

Altogether, these results suggest that the inclusion of Gua affects the sugar puckering. This is not surprising, given that quadruplexes are known to exhibit enhanced flexibility following the loss of phosphate groups from GMP molecules [1,37], resulting in bending and folding of the cylinders. As a consequence of this higher flexibility, the sugar moieties may potentially be force to the acquisition of distinct conformations.

3.3.5. Phosphate groups

In the IR absorbance spectrum of GMP/K, a prominent band at 1060 cm^{-1} was observed, corresponding to the 1067 cm^{-1} and 1050 cm^{-1} s derivative peaks and reported to be assigned to the symmetric stretching vibration of phosphate groups. Both the absorbance and second derivative IR spectra show that the increasing Gua:GMP ratio is clearly related to a significant decrease in the intensity of these peaks, consistently with a decrease in the relative amount of phosphate groups within the binary Gua/GMP samples (Fig. 12).

Moreover, the band centered at 966 cm^{-1}, mainly assigned to the PO_3^{2-} group vibration, displayed a significant decrease in its intensity, as expected. This peak also underwent a blue shift, from 966 cm^{-1} in GMP/K and 1:4 Gua:GMP, to 968 cm^{-1} of 1:2 Gua:GMP and 1:2 Gua:GMP, to 972 cm^{-1} of 3:2 Gua:GMP.

3.4. Gua:GMP/Na quadruplexes: composition effects on the mid-IR spectra

With the same approach, the changes in the spectral profile induced by the increasing Gua:GMP ratio were evaluated also for GMP/Na. The 3:2 Gua:GMP/Na sample was not included, since it was highly unstable and separated before measurements [7].

Respect to GMP/K, the differences in the spectral profile attributable to Gua inclusion were not striking, as reported in Fig. C.19 in Appendix C. Conversely, the 1200–915 cm^{-1} spectral ranges resulted to be affected by the mixing of GMP/Na with Gua (Fig. 13). Indeed, the lack of phosphate groups following the inclusion of Gua molecules into the quartets and quadruplexes determined the same changes found for GMP/K. In particular, the intensity decrease of the bands at ~1060 cm^{-1} and ~966 cm^{-1}, assigned to the vibrations of the phosphate groups, appears related to the increasing Gua:GMP ratio.

4. Conclusions

Given their unique properties, including bio-compatibility, self-healing, injectability, stability, and orientational persistence, self-assembling guanine hydrogels have been considered for different

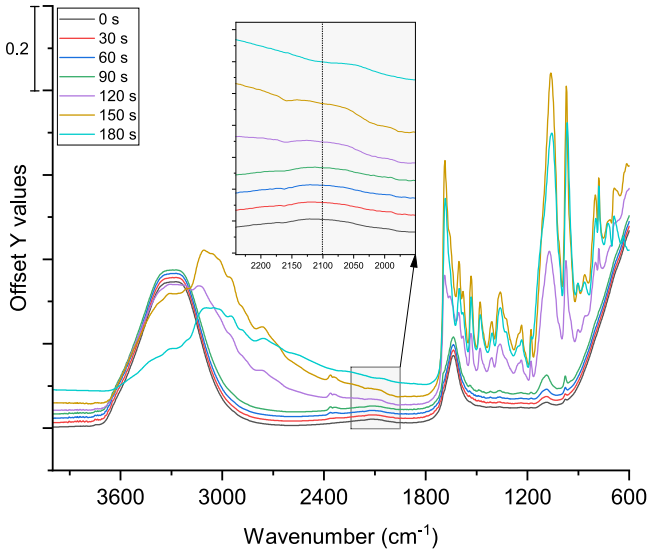

Fig. A.14. Representative infrared spectra of 1:2 GMP/K acquired every 30 s until complete dehydration.

applications in bio-nanotechnology, biomedical engineering, and 3D bio-printing technology [36,38,39]. However, the evaluation of the potential applications need a complete understanding of the structural and chemical-physical properties of the supramolecular structures at all the different degree of complexity. Therefore, this paper focuses on the analysis by ATR-FTIR spectroscopy of the vibrational characteristics of guanosine aggregates forming in water, from the G-quartets to the G-quadruplexes and the G-hydrogels.

The characteristic vibrational spectrum of the quadruplex structure of GMP/K in water was firstly investigated: the identified peaks reflect the chemical composition but also the formation of quartets, octamers, and quadruplexes. The comparison with spectra obtained using GMP/Na then confirmed the different role of K^+ and Na^+ cations in promoting the quadruplex formation: potassium ions induce a larger stabilization of the G-quadruplex organization. Finally, hydrogels prepared in water using binary mixtures of Gua and GMP/K or Gua and GMP/Na were considered. As a result, the same G-quadruplex-based structure was found in both mixtures, but the Gua/GMP ratio affects important chemical-physical features, like sugar puckering, guanine vibrations, and base stacking, which together reflect the known side-to-side aggregation and bundle formation occurring in such a system.

This work demonstrates the significant capability of infrared spectroscopy in the study of guanosine-derived hydrogels, offering crucial insights at the molecular and chemical levels that are not typically accessible through conventional experimental techniques used for such systems. Indeed, an in-depth comprehension of the molecular mechanism underlying quadruplex formation as a function of the environment (K^+/Na^+ cations) or of the hydrogel composition (Gua:GMP molar ratio) is of undoubted importance in the design and fabrication of a smart material with tunable properties for biotechnological and biomedical applications.

CRediT authorship contribution statement

Valentina Notarstefano: Writing – review & editing, Writing – original draft, Methodology, Investigation, Formal analysis, Data curation. **Alessia Pepe:** Writing – original draft, Methodology, Investigation, Formal analysis. **Francesca Ripanti:** Writing – original draft, Methodology, Formal analysis, Data curation. **Federica Piccirilli:** Writing – review & editing, Methodology, Formal analysis, Data curation. **Lisa Vaccari:** Writing – review & editing, Methodology, Formal analysis, Data curation. **Paolo Mariani:** Writing – review & editing, Supervision, Resources, Project administration, Methodology, Funding acquisition, Conceptualization.

Declaration of competing interest

The authors declare the following financial interests/personal relationships which may be considered as potential competing interests: Valentina Notarstefano reports financial support was provided by European Union. Paolo Mariani reports financial support was provided by European Union. The other authors declare that they have no known competing financial interests or personal relationships that could have appeared to influence the work reported in this paper.

Data availability

Data will be made available on request.

Acknowledgments

This research has received funding from the project Vitality – Project Code ECS00000041, CUP I33C22001330007 - funded under the National Recovery and Resilience Plan (NRRP), Mission 4 Component 2 Investment 1.5 - 'Creation and strengthening of innovation ecosystems,' construction of 'territorial leaders in R&D' – Innovation Ecosystems - Project 'Innovation, digitalization and sustainability for the diffused economy in Central Italy – VITALITY' Call for tender No. 3277 of 30/12/2021, and Concession Decree No.0001057.23-06-2022 of Italian Ministry of University funded by the European Union – NextGenerationEU.

This work has been partially funded by the project funded under the National Recovery and Resilience Plan (NRRP), Mission 4 Component 2 Investment 1.4 - Call for tender No. 3138 of 16 December 2021, rectified by Decree n. 3175 of 18 December 2021 of Italian Ministry of University and Research funded by the European Union – NextGenerationEU; award Number: Project code CN_00000033, Concession Decree No. 1034 of 17 June 2022 adopted by the Italian Ministry of University and Research, CUP I33C22001300007 Project title "National Biodiversity Future Center — NBFC".

Appendix A. Sample dehydration

As described in the Experimental section, samples were deposited onto the diamond crystal and purged with a continuous stream of nitrogen gas for the complete removal of the free water content, which was monitored by checking the disappearance of the band at ~2100 cm^{-1} originated from the free water content (Fig. A.14).

Appendix B. Gua and GMP powder spectra

For completeness, Gua and GMP (GMP disodium salt) powder IR spectra were also acquired, in order to validate the obtained results. Representative spectra are shown in Fig. B.15 in the most significant spectral range.

For example, only in Gua sample, a band centered at 1725 cm^{-1} was found: this is ascribable to vibrations of the –COOH moiety, absent when the phosphate group is present. Similarly, a peak at ~915 cm^{-1}, ascribable to the –OH wagging of the carboxylic moiety, was found only in Gua. The $\nu_{C6=O6}$ peak, centered at ~1685 cm^{-1} in GMP/Na in solution, was found at ~1670 cm^{-1} both in Gua and GMP/Na powders, confirming the lack of guanosine self-association. Conversely, a peak at ~1620 cm^{-1} was detected in Gua and GMP/Na powder samples, while it was absent in solution: this peak is reported to be

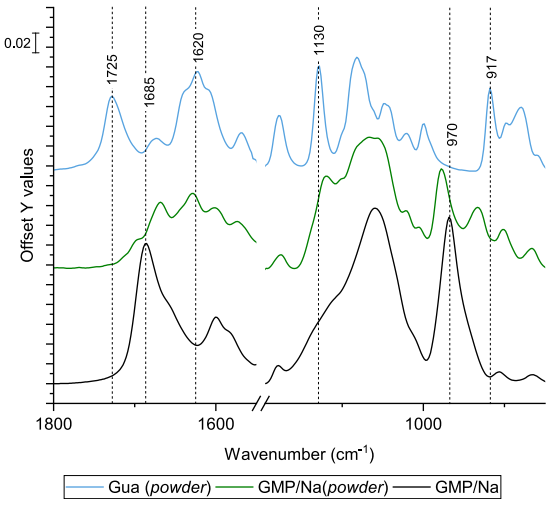

Fig. B.15. Infrared spectra of Gua (powder), GMP/Na (powder), and GMP/Na (solution) in the most representative spectral ranges.

Table C.1
Principal parameters of Gaussian functions used for fitting spectra of GMP/K and GMP/Na in the 1730–1550 cm^{-1} spectral range. Spectra were subjected to vector normalization in the two different sub-regions (1730–1620 cm^{-1} and 1630–1550 cm^{-1}).

	GMP/K	GMP/Na
x_c [cm^{-1}]	1686.0 ± 0.5	1688.0 ± 0.5
A [cm^{-2}]	2.99 ± 0.01	2.95 ± 0.01
w [cm^{-1}]	25.0 ± 0.1	25.7 ± 0.1
x_c [cm^{-1}]	1660.0 ± 0.5	1662.0 ± 0.5
A [cm^{-2}]	2.13 ± 0.01	1.99 ± 0.01
w [cm^{-1}]	34.0 ± 0.3	36.1 ± 0.3
x_c [cm^{-1}]	1603.0 ± 0.5	1600.0 ± 0.5
A [cm^{-2}]	0.81 ± 0.01	0.65 ± 0.02
w [cm^{-1}]	20.9 ± 0.2	19.2 ± 0.4
x_c [cm^{-1}]	1580.0 ± 0.5	1582.0 ± 0.5
A [cm^{-2}]	0.3 ± 0.1	0.47 ± 0.02
w [cm^{-1}]	15 ± 1	21 ± 1
x_c [cm^{-1}]	1570.0 ± 0.5	–
A [cm^{-2}]	0.2 ± 0.1	–
w [cm^{-1}]	20 ± 1	–

related to base carbonyl stretching and ring breathing mode, which may be inhibited upon quartet and quadruplex formation. Similarly, the peak at ~1130 cm^{-1}, prominent in Gua, less in GMP/Na powder, and almost invisible in the absorbance spectrum of GMP/Na in solution, is ascribable to ring breathing modes of ribose. Finally, as expected, the phosphate-related peak at ~970 cm^{-1} was absent in the spectrum of Gua powder.

Appendix C. Spectrum deconvolution fit details

In this section, the details of the careful fitting analysis are reported. As stated in Material and Methods section, experimental spectra were fitted through a combination of Gaussian curves ($y = y_0 + \frac{A}{w\sqrt{\pi/2}} e^{-2\frac{(x-x_c)^2}{w^2}}$) where x_c represents the center of the band, A its intensity calculated as the integrated area under the curve, and w its width obtained as full width at half maximum, in order to quantify the

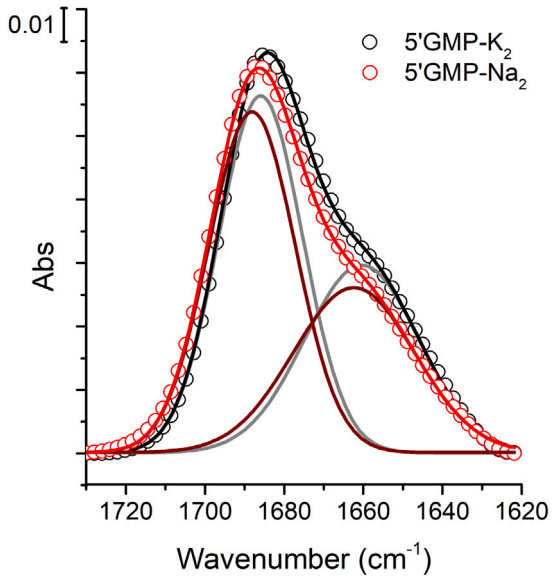

Fig. C.16. Details of fitting results in the 1730–1620 cm^{-1} spectral region for both GMP/K (black) and GMP/Na (red): the experimental spectra (empty dots) were deconvolved through Gaussian functions (gray curves for GMP/K and wine for GMP/Na) obtaining the fitting curve (black and red for GMP/K and GMP/Na respectively).

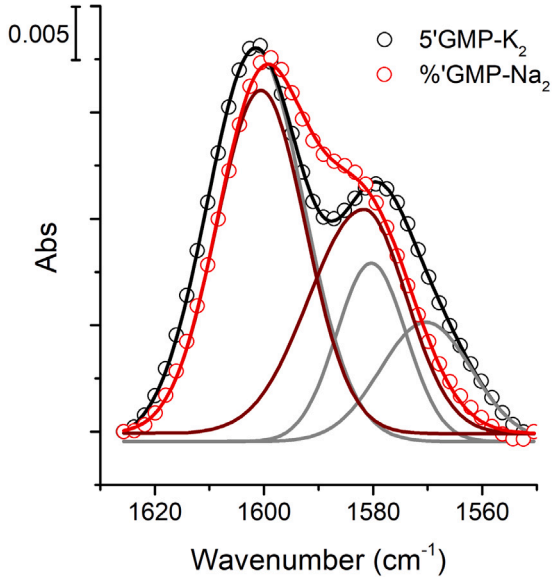

Fig. C.17. Details of fitting results in the 1630–1550 cm^{-1} spectral region for both GMP/K (black) and GMP/Na (red): the experimental spectra (empty dots) were deconvolved through Gaussian functions (gray curves for GMP/K and wine for GMP/Na) obtaining the fitting curve (black and red for GMP/K and GMP/Na respectively).

spectral differences due to the environment and hydrogel composition. In particular, the comparison of the fitting results from GMP in the diverse cations are shown in Figs. C.16 and C.17 in the 1730–1620 cm^{-1} and 1630–1550 cm^{-1}, respectively. The principal fitting parameters are reported in Table C.1.

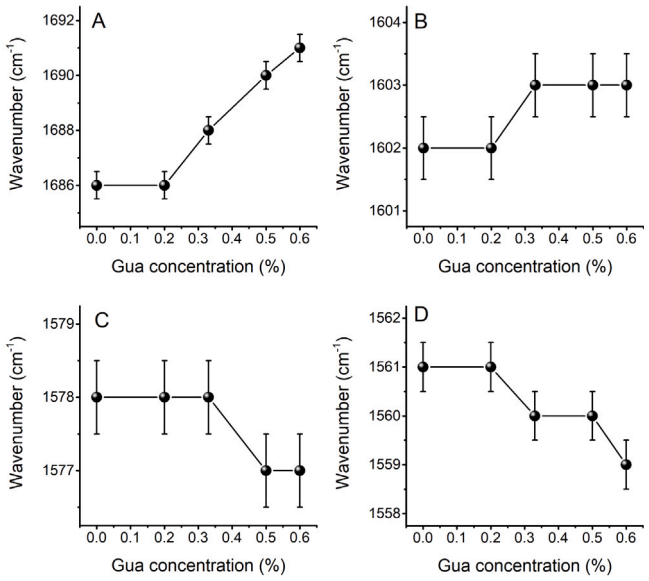

Fig. C.18. Center position of the principal peaks in the 1700–1550 cm^{-1} spectral region of GMP/K and Gua:GMP/K at different molar ratio as a function of Gua concentration. Errors come from Gaussian deconvolution fit.

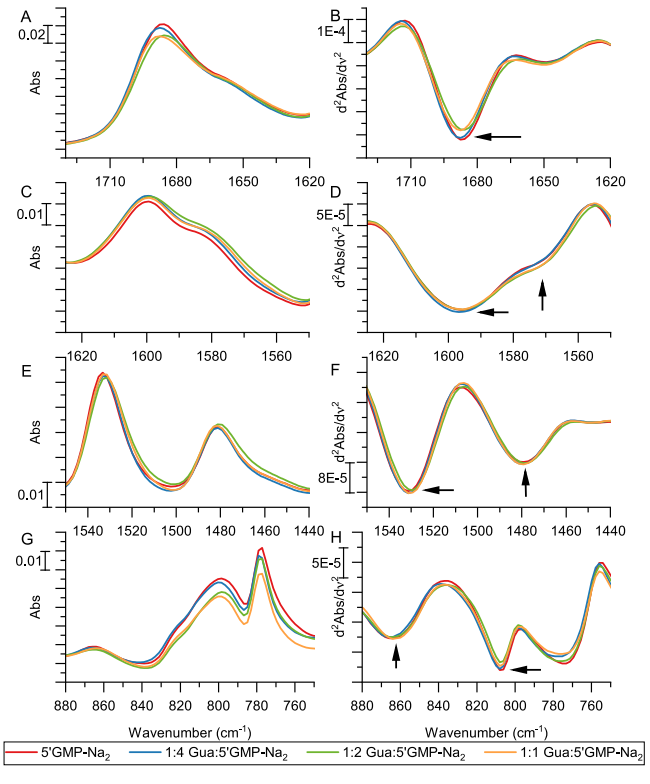

Fig. C.19. Comparison of the spectral profiles of GMP/Na (red), 1:4 Gua:GMP/Na (cyan), 1:2 Gua:GMP/Na (green), and 1:1 Gua:GMP/Na (orange) in the 1725–1620 cm^{-1} (A, absorbance; B, second derivative), in the 1625–1550 cm^{-1} (C, absorbance; D, second derivative), in the 1550–1440 cm^{-1} (E, absorbance; F, second derivative), and in the 880–770 cm^{-1} (G, absorbance; H, second derivative) spectral ranges.

References

[1] F. Carducci, J.S. Yoneda, R. Itri, P. Mariani, On the structural stability of guanosine-based supramolecular hydrogels, Soft Matter 14 (15) (2018) 2938–2948, http://dx.doi.org/10.1039/C8SM00299A.

[2] P. Mariani, C. Mazabard, A. Garbesi, G.P. Spada, A study of the structure of the lyomesophases formed by the dinucleoside phosphate d(GpG). An approach by x-ray diffraction and optical microscopy, J. Am. Chem. Soc. 111 (16) (1989) 6369–6373, http://dx.doi.org/10.1021/ja00198a057.

[3] P. Mariani, L. Saturni, Measurement of intercolumnar forces between parallel guanosine four-stranded helices, Biophys. J. 70 (6) (1996) 2867–2874, http://dx.doi.org/10.1016/S0006-3495(96)79856-9.

[4] L.I. Jansson, J. Hentschel, J.W. Parks, T.R. Chang, C. Lu, R. Baral, C.R. Bagshaw, M.D. Stone, Telomere DNA G-quadruplex folding within actively extending human telomerase, Proc. Natl. Acad. Sci. 116 (19) (2019) 9350–9359, http://dx.doi.org/10.1073/pnas.1814777116.

[5] P. Mariani, F. Ciuchi, L. Saturni, Helix-specific interactions induce condensation of Guanosine four-stranded helices in concentrated salt solutions, Biophys. J. 74 (1) (1998) 430–435, http://dx.doi.org/10.1016/S0006-3495(98)77800-2.

[6] Y. Du, T. Liu, F. Tang, X. Jin, H. Zhao, J. Liu, X. Zeng, Q. Chen, Chirality from D-guanosine to L-guanosine shapes a stable gel for three-dimensional cell culture, Chem. Commun. 57 (96) (2021) 12936–12939, http://dx.doi.org/10.1039/C9CC09911E.

[7] A. Pepe, P. Moretti, J.S. Yoneda, F. Carducci, R. Itri, P. Mariani, Self-oriented anisotropic structure of G-hydrogels as a delicate balance between attractive and repulsive forces, Nanoscale 15 (37) (2023) 15196–15205, http://dx.doi.org/10.1039/D3NR01348K.

[8] E.J. Baldassarri, M.G. Ortore, F. Spinozzi, A. Round, C. Ferrero, P. Mariani, K+ vs. Na+ effects on the self-assembly of Guanosine 5'-Monophosphate: A solution SAXS structural study, Nanomaterials 10 (4) (2020) 629, http://dx.doi.org/10.3390/nano10040629.

[9] M.R. Guzmán, J. Liquier, S. Brahmachari, E. Taillandier, Characterization of parallel and antiparallel G-tetraplex structures by vibrational spectroscopy, Spectrochim. Acta A 64 (2) (2006) 495–503, http://dx.doi.org/10.1016/j.saa.2005.07.049.

[10] J.A. Mondragón-Sánchez, J. Liquier, R.H. Shafer, E. Taillandier, Tetraplex structure formation in the Thrombin-binding DNA aptamer by metal cations measured by vibrational spectroscopy, J. Biomol. Struct. Dyn. 22 (3) (2004) 365–373, http://dx.doi.org/10.1080/07391102.2004.10507008.

[11] M. Gao, B. Harish, M. Berghaus, R. Seymen, L. Arns, S.A. McCallum, C.A. Royer, R. Winter, Temperature and pressure limits of guanosine monophosphate self-assemblies, Sci. Rep. 7 (1) (2017) 9864, http://dx.doi.org/10.1038/s41598-017-10689-0.

[12] B.C. Smith, The carbonyl group, part I: Introduction, Spectroscopy 32 (9) (2017) 31–36.

[13] D.A. Price, Z.J. Kartje, J.A. Hughes, T.D. Hill, T.M. Loth, J.K. Watts, K.T. Gagnon, S.D. Moran, Infrared spectroscopy reveals the preferred motif size and local disorder in parallel stranded DNA G-Quadruplexes, ChemBioChem 21 (19) (2020) 2792–2804, http://dx.doi.org/10.1002/cbic.202000136.

[14] V. Andrushchenko, P. Bouř, Infrared absorption detection of metal ion-deoxyguanosine monophosphate binding: Experimental and theoretical study, J. Phys. Chem. B 113 (1) (2009) 283–291, http://dx.doi.org/10.1021/jp8058678.

[15] Y. Li, X. Han, S. Zhou, Y. Yan, X. Xiang, B. Zhao, X. Guo, Structural features of DNA G-Quadruplexes revealed by surface-enhanced Raman spectroscopy, J. Phys. Chem. Lett. 9 (12) (2018) 3245–3252, http://dx.doi.org/10.1021/acs.jpclett.8b01353.

[16] H.R. Paudel, R. Das, C.-H. Wu, J.I. Wu, Self-assembling purine and pteridine quartets: how do π-conjugation patterns affect resonance-assisted hydrogen bonding? Org. Biomol. Chem. 18 (6) (2020) 1078–1081, http://dx.doi.org/10.1039/C9OB02412C.

[17] P. Audet, C. Simard, R. Savoie, A vibrational spectroscopic study of the self-association of 5'-GMP in aqueous solution, Biopolymers 31 (2) (1991) 243–251, http://dx.doi.org/10.1002/bip.360310211.

[18] A.T. Krummel, M.T. Zanni, DNA vibrational coupling revealed with two-dimensional infrared spectroscopy: Insight into why vibrational spectroscopy is sensitive to DNA structure, J. Phys. Chem. B 110 (28) (2006) 13991–14000, http://dx.doi.org/10.1021/jp062597w.

[19] V. Gabelica, F. Rosu, E. De Pauw, J. Lemaire, J.-C. Gillet, J.-C. Poully, F. Lecomte, G. Grégoire, J.-P. Schermann, C. Desfrançois, Infrared signature of DNA G-quadruplexes in the gas phase, J. Am. Chem. Soc. 130 (6) (2008) 1810–1811, http://dx.doi.org/10.1021/ja077321w.

[20] D.A. McGovern, S. Quinn, G.W. Doorley, A.M. Whelan, K.L. Ronayne, M. Towrie, A.W. Parker, J.M. Kelly, Picosecond infrared probing of the vibrational spectra of transients formed upon UV excitation of stacked G-tetrad structures, Chem. Commun. (48) (2007) 5158, http://dx.doi.org/10.1039/b711172j.

[21] V. Andrushchenko, D. Tsankov, M. Krasteva, H. Wieser, P. Bouř, Spectroscopic detection of DNA quadruplexes by vibrational circular dichroism, J. Am. Chem. Soc. 133 (38) (2011) 15055–15064, http://dx.doi.org/10.1021/ja204630k.

[22] M. Mathlouthi, A.M. Seuvre, J.L. Koenig, F.T.-I.R. and laser-raman spectra of guanine and guanosine, Carbohydr. Res. 146 (1) (1986) 15–27, http://dx.doi.org/10.1016/0008-6215(86)85020-0.

[23] H.A. Tajmir-Riahi, T. Theophanides, A Fourier transform infrared study of the electrophilic attack at the N7-site of guanosine-5'-monophosphate, Can. J. Chem. 62 (2) (1984) 266–272, http://dx.doi.org/10.1139/v84-044.

[24] M. Banyay, M. Sarkar, A. Gräslund, A library of IR bands of nucleic acids in solution, Biophys. Chem. 104 (2) (2003) 477–488, http://dx.doi.org/10.1016/S0301-4622(03)00035-8.

[25] G. Wu, I.C.M. Kwan, Helical structure of disodium 5'-Guanosine monophosphate self-assembly in neutral solution, J. Am. Chem. Soc. 131 (9) (2009) 3180–3182, http://dx.doi.org/10.1021/ja809258y.

[26] G. Wu, I.C.M. Kwan, Z. Yan, Y. Huang, E. Ye, On the helical structure of Guanosine 5'-monophosphate formed at pH 5: Is it left- or right-handed? J. Nucleic Acids 2017 (2017) e6798759, http://dx.doi.org/10.1155/2017/6798759.

[27] J.T. Davis, G-Quartets 40 years later: From 5'-GMP to molecular biology and supramolecular chemistry, Angew. Chem., Int. Ed. 43 (6) (2004) 668–698, http://dx.doi.org/10.1002/anie.200300589.

[28] E. Taillandier, J. Liquier, Vibrational spectroscopy of nucleic acids, in: J.M. Chalmers, P.R. Griffiths (Eds.), Handbook of Vibrational Spectroscopy, first ed., Wiley, 2001, http://dx.doi.org/10.1002/0470027320.s8204.

[29] B.R. Wood, The importance of hydration and DNA conformation in interpreting infrared spectra of cells and tissues, Chem. Soc. Rev. 45 (7) (2016) 1980–1998, http://dx.doi.org/10.1039/C5CS00511F.

[30] A.C.S. Talari, M.A.G. Martinez, Z. Movasaghi, S. Rehman, I.U. Rehman, Advances in Fourier transform infrared (FTIR) spectroscopy of biological tissues, Appl. Spectrosc. Rev. 52 (5) (2017) 456–506, http://dx.doi.org/10.1080/05704928.2016.1230863.

[31] K. Mudroňová, V. Římal, P. Mojzeš, Effect of ribose versus 2'-deoxyribose residue in guanosine 5'-monophosphates on formation of G-quartets stabilized by potassium and sodium cations, Vib. Spectrosc. 82 (2016) 60–65, http://dx.doi.org/10.1016/j.vibspec.2015.12.002.

[32] A. Messinger, J.W. Powell, T. Weidlich, L. Genzel, Far-Infrared study of the vibrational modes of 5'-GMP gels and crystals of Na+ and K+, J. Biomol. Struct. Dyn. 10 (5) (1993) 841–852, http://dx.doi.org/10.1080/07391102.1993.10508678.

[33] J. Gu, J. Leszczynski, Origin of Na+/K+ selectivity of the guanine tetraplexes in water: The theoretical rationale, J. Phys. Chem. A 106 (3) (2002) 529–532, http://dx.doi.org/10.1021/jp012739g.

[34] D. Bhattacharyya, G. Mirihana Arachchilage, S. Basu, Metal cations in G-quadruplex folding and stability, Front. Chem. 4 (2016) http://dx.doi.org/10.3389/fchem.2016.00038.

[35] Y. Yu, D. Nakamura, K. DeBoyace, A.W. Neisius, L.B. McGown, Tunable thermoassociation of binary Guanosine gels, J. Phys. Chem. B 112 (4) (2008) 1130–1134, http://dx.doi.org/10.1021/jp709613p.

[36] J.S. Yoneda, D.R. De Araujo, F. Sella, G.R. Liguori, T.T. Liguori, L.F.P. Moreira, F. Spinozzi, P. Mariani, R. Itri, Self-assembled guanosine-hydrogels for drug-delivery application: Structural and mechanical characterization, methylene blue loading and controlled release, Mater. Sci. Eng.: C 121 (2021) 111834, http://dx.doi.org/10.1016/j.msec.2020.111834.

[37] G. Nava, F. Carducci, R. Itri, J.S. Yoneda, T. Bellini, P. Mariani, Quadruplex knots as network nodes: Nano-partitioning of Guanosine derivates in supramolecular hydrogels, Soft Matter 15 (1) (2019) 2315–2318, http://dx.doi.org/10.1039/C8SM02616E.

[38] Y. Li, J. Chi, P. Xu, X. Dong, A.-T. Le, K. Shi, Y. Liu, J. Xiao, Supramolecular G-quadruplex hydrogels: Bridging fabrication to biomedical application, J. Mater. Sci. Technol. (2023).

[39] M. Godoy-Gallardo, M. Merino-Gómez, M.A. Mateos-Timoneda, U. Eckhard, F.J. Gil, R.A. Perez, Advanced binary guanosine and guanosine 5'-monophosphate cell-Laden hydrogels for soft tissue reconstruction by 3D bioprinting, ACS Appl. Mater. Interfaces 15 (25) (2023) 29729–29742.